Journal of Applied Phycology (2026) 38:1549–1564
https://doi.org/10.1007/s10811-025-03772-x

RESEARCH

Integrated extraction, film formulation, and physicochemical comparison of crude carrageenans from *Mastocarpus stellatus*: Exploring enzymatic, hydrothermal, and ultrasonication pathways

K. L. Baltrusch[1] · M. D. Torres[1] · H. Domínguez[1]

Received: 29 July 2025 / Revised: 19 December 2025 / Accepted: 24 December 2025 / Published online: 9 February 2026
© The Author(s) 2026

Abstract
This study evaluated various extraction pathways for crude carrageenan extraction (CCAR) from *Mastocarpus stellatus* (Stackhouse) Guiry, using combinations of hydrothermal-, enzymatic- (Cellic® CTec3), and ultrasound (US)-assisted extractions. Extraction yield, purity, chemical composition, structural features, film and gel rheology were assessed to guide an integrated seaweed biorefinery design. Hydrothermal-assisted extraction yielded CCAR with a low ash content of 17% (d.w.) and an apparent molecular weight (M_w) of 1087 kDa, though recovery was limited (11.1%). Enzymatic extraction (CCAR-6) achieved the highest CCAR yield (38.5% d.w.) while maintaining relatively high M_w (1210 kDa). Combined enzyme-US extractions resulted in CCAR recovery up to 33.5% d.w. but with increased ash and protein contents, especially in carrageenan recovered from solid residue extracts (e.g., CCAR-7: 35.5% ash, 6.1% protein; d.w.). Gels from CCAR with low contamination and high apparent M_w, tended to higher complex viscosity. Conversely, gels derived from low M_w or high-ash CCARs, showed lower complex viscosity. Rheological analysis of carrageenan films with PEG600 revealed correlations between extract purity, and viscoelastic performance, although no clear effect of M_w could be distiguished. Overall, the results underscore the impact of different extraction technologies on CCAR functionality and purity, as well as potential of solid residues, providing a foundation for efficient and sustainable extraction protocols in macroalgal biorefineries.

Keywords *Mastocarpus stellatus* · Rhodophta · Ultrasound · Enzyme · Hydrothermal extraction · Carrageenan

Introduction

Sulfated polysaccharides represent the polysaccharidic soluble fraction of seaweeds and usually operate as structural components of the algal cell walls. There, they form a matrix together with cellulose fibrils and proteins, contributing to the structural flexibility of seaweeds and enhancing their adaptability to both physical and biotic stresses (Miller and Blunt 2002; Michel et al. 2010; Domozych et al. 2012; Li et al. 2025). Concentration and structure of these polysaccharides varies both depending on their ecophysiological context and specific life stage (Shepherd et al. 1999; Andrade et al. 2010; Tasende et al. 2013; Skriptsova 2016; Sfriso et al. 2017). Due to their unique properties of biocompatibility and biodegradability, these natural carbohydrates are increasingly used either in their native form or after chemical modification. Furthermore, they are highly appreciated as valuable ingredients of biomaterials, with potential in the biomedical field (Morelli et al. 2017; Andryukov et al. 2020; Shen et al. 2021; Ramos-de-la-Peña et al. 2022; Farshidfar et al. 2023; Lomartire and Gonçalves 2023; Sabu Mathew et al. 2024).

In red seaweeds (Rhodophyta), agars and carrageenans are the main representatives of sulfated polysaccharides. Carrageenans are linear polysaccharides, mainly composed of repeating units of α-D-galactopyranose (1→3 linked) and β-D-galactopyranose (1→4 linked) (Azevedo et al. 2013). In gelling carrageenans such as κ- and ι-types, the 4-linked galactose residue is converted into a 3,6-anhydrogalactose unit, forming an intramolecular anhydro bridge. This structural feature adopts the $^1C_4$ chair conformation, which is essential for establishing the helical structure that enables gel formation. In contrast, λ-carrageenan and its precursor

✉ M. D. Torres
matorres@uvigo.gal

[1] Department of Chemical Engineering, CINBIO, Universidade de Vigo, Campus Ourense, Edificio Politécnico, As Lagoas s/n, 32004 Ourense, Spain

forms (μ- and *ν*-carrageenans) lack the 3,6-anhydro bridge; consequently, their 4-linked residues adopt the $^4C_1$ chair conformation, which disrupts helix formation and prevents gelation (Pereira and Van De Velde 2011). In addition, carrageenan also contains sulfate hemiester groups, as well as methoxy and pyruvate substitutes (Hettle et al. 2018).

Preliminary studies revealed a common array of biological properties displayed by carrageenans both *in vitro* and *in vivo* (Patel 2012). Most of the biological properties of carrageenans were attributed to the presence of sulfate groups. Especially the position occupied by sulfate groups rather than the amount present within the chemical structure of the polysaccharide was found to be determinant (de Araújo et al. 2013). Carrageenans are commonly used as a thickener and stabilizer in food products, recognized by EU additive codes E407 for refined and E407a for semi-refined carrageenan. It is also a generaly regarded as safe (GRAS) food additive per FDA regulations (U.S. Food and Drug Administration 2025), and is generaly considered a non-organic additive in organic food products, as per both U.S. and EU regulations. In the EU, carrageenan is included in the Implementing Regulation (EU) 2021/1165, which lists substances authorized for use in organic production. While carrageenan is permitted in organic food processing, it is currently not eligible for organic certification itself (The European Commission 2021). Similarly, the U.S. Department of Agriculture (USDA) has included carrageenan on the National List of Allowed Non-Organic Substances, meaning it can be used in products labeled as 'organic' when no organic alternative exists (U.S. Department of Agriculture 2025).

Carrageenan that is extracted through physical methods (such as heating, mechanical agitation, or ultrasonication) without the use of chemical reagents from organically cultivated seaweeds may be considered for organic certification in the future. Enzymatic extraction may also be acceptable if the enzymes employed are approved for organic processing (The European Commission 2021). In contrast, carrageenan obtained via alkaline or other chemical treatments is considered chemically modified and therefore not certifiable as organic, although it remains permitted as a non-organic additive in certified organic products.

Carrageenan has also recently attracted interest for food packaging applications, as its compatibility with other biopolymers and potential for active packaging make it a promising material for extending shelf life (Sabu Mathew et al. 2024). The biodegradability and affordability of carrageenan-based films make them a promising alternative to plastic packaging (Cheng et al. 2022). The global carrageenan industry was valued at approximately US$ 924.7 million in 2023 and is projected to grow at about 5.4% until 2030 (Zhang et al. 2023).

In a context of an increasing demand for more sustainable production techniques, there is a growing interest for research into greener pathways for carrageenan production. In this context, alternative extraction methods as hydrothermal-assisted (Flórez-Fernández et al. 2022), ultrasonic (Torres et al. 2021) or enzymatically-assisted (Blanco-Pascual et al. 2014) extraction methods have been proposed as eco-efficient alternatives to conventional alkaline-based methods, which are energy-intensive, require large volumes of solvents, and take long processing times, while also generating hazardous effluents that pose environmental and regulatory challenges (ICF International 2011; Abdul Khalil et al. 2018; Matos et al. 2021). Nevertheless, despite their environmental advantages, these alternative methods are still at the laboratory or pilot scale, and their implementation at industrial levels remains technically and economically unfeasible at present. The physicochemical properties of carrageenans, such as purity, molecular weight or sulfation, are strongly influenced by the employed extraction method (Ferdiansyah et al. 2023; Mendes et al. 2024). Moreover, comparing carrageenan from different studies is challenging due to the inherent variability in macroalgal raw material, which is influenced not only by species differences but also by eco-physiological conditions and life stages (Shepherd et al. 1999; Andrade et al. 2010; Skriptsova 2016; Sfriso et al. 2017). Therefore, conducting a systematic comparison of green extraction methods using a single macroalgal source is essential for accurately assessing how different techniques affect the structural and functional properties of the final carrageenan product. In addition, solid residues from extraction processes frequently contain important amounts of residual carrageenan (Bianchi et al. 2022) highlighting the need to explore their potential for further valorization.

In this line, the main aim of this study was to evaluate and compare different green strategies for extracting crude carrageenan from the gametophyte of the edible red seaweed *Mastocarpus stellatus*, with a focus on integrating hydrothermal-, enzymatic- and ultrasound-assisted processes to improve yield and maximize carrageenan recovery both from the starting biomass and the solid residue. Additionally, the commercial enzyme mix Cellic® CTec3 was applied for the first time to carrageenan extraction. The extracted carrageenans were thoroughly characterized in terms of purity, composition, physicochemical properties, and their functional performance in gel formation and film development was analyzed.

Materials and methods

Raw materials

Mature, healthy gametophytes of *Mastocarpus stellatus* were randomly collected by hand from the intertidal zone along the Galician coast (NW Spain). Although the exact

collection sites were not specified, the samples were kindly provided by Porto-Muíños S.L. (A Coruña, Spain). The material was supplied in a dried state. We note that while *M. stellatus* has a triphasic heteromorphic life cycle (Tasende et al. 2013), the samples analyzed mainly correspond to gametophytes, as tetrasporophytes occur as a crustose form. The carposporophyte phase may also be present on gametophyte females but, given its small size, it is unlikely to significantly affect carrageenan content. Samples were milled with an A320 chopper (Moulinex, Spain), until a particle size below 0.5 cm was obtained.

Extraction techniques and polysaccharide recovery

For hydrothermal extraction a pressurized stirred reactor (Parr Instr., USA) was used, with a liquid-to-solid ratio of 20:1 (w:w), using water as only solvent. The treatment consisted of a non-isothermal heating process, where the temperature was raised to 130 ºC based on the optimum obtained in previous studies (Flórez-Fernández et al. 2022), after which reactor was cooled down to 60 ºC before beeing opened. Pressure during the reaction was autogenous and approximately 758 kPa. Extraction time was approximately 30 min.

Ultrasound-assisted extraction is based on the formation of cavitation bubbles, that cause high shear pressure which disrupts cell walls, allowing the dissolution of seaweed compounds into the solvent, often water (Qiu et al. 2022; Baltrusch et al. 2025). An ultrasonic bath (Fisherbrand Scientific, FB11207) was used, set at 100% amplitude, 37 kHz frequency, 1130 W power, and a constant temperature of 55 ºC. Extraction times ranged from 1 to 3 hours and were performed without stirring.

Enzyme-assisted extraction used the Cellic® CTec3 enzyme complex, generously provided by Novozymes (Denmark). This complex exhibits cellulase, hemicellulase, and β-glucosidase activities and is commonly employed in the processing of lignocellulosic materials (Silveira et al. 2018). The enzyme activity, measured by filter paper assay, was 183 FPU mL^{-1}. A dosage of 300 µL of Cellic® CTec3 (which corresponds to 10 mg of enzymes) per gram of dry seaweed was applied. Extraction conditions were set to 55 °C, pH 5.6, 300 mM NaCl, and 50 mM acetate buffer, with a solid-to-liquid ratio of 1:30, following conditions similar to those previously described (Rhein-Knudsen et al. 2023; Baltrusch et al. 2024). The reactions were terminated by heating the filtered extract to 95 °C for 5 min. This dosage was selected to evaluate the enzymatic potential rather than its immediate industrial feasibility. It is acknowledged that, at large production scales, such enzyme loads would require optimization or enzyme-recycling strategies to become economically viable.

All extractions were performed at least in triplicate. Residual solid phases were separated through membrane vacuum filtration with filter paper and convective air-dried at 40 ºC in an oven until constant weight. Carrageenan fractions were isolated from the obtained extracts liquid phases by precipitation with 96% ethanol (at an extract:ethanol ratio of 1:2). To recover the carrageenan, the precipitates were subjected to gauze filtration, washed twice with 96% ethanol, and subsequently convective air-dried at 40 ºC for 24 h. Afterwards, crude carrageenan samples were ground with a hand mortar, before beeing used in further experiments or analysis. Crude carrageenan obtention yield was calculated as the percentage of dry crude carrageenan recovered after precipitation, relative to the initial dry weight of the biomass. All yields reported in this study refer to crude carrageenan-rich extracts, which were not subjected to further purification. These values therefore represent total extractable polysaccharides obtained under each condition, including naturally associated ash and protein fractions.

Proximate composition analysis of crude carrageenans

Moisture content was determined gravimetrically by drying the samples at 105 °C until constant weight. Ash content was measured by calcination at 575 °C. Protein content was estimated based on total nitrogen quantification using the Kjeldahl method, applying a specific nitrogen-to-protein conversion factor of 4.59 for red seaweeds (Lourenço et al. 2002). Alkali-extracted commercial carrageenan (Sigma-Aldrich, USA) was used as control for comparison. All measurements were performed at least in triplicate.

FT-IR spectroscopy

Fourier transform infrared spectroscopy with attenuated total reflectance (FTIR-ATR) was conducted using a Nicolet 6700 spectrometer (Fisherbrand Scientific, Canada). A high refractive index crystal (diamond) was used as the ATR element. Spectra were collected at room temperature with a resolution of 4 cm^{-1} and a scanning rate of 32 scans per min. The spectral range covered 400 to 4000 cm^{-1}. All measurements were performed in triplicate to ensure data reliability. This analysis was used to qualitatively assess the chemical characteristics of the dried extracts.

Proton nuclear magnetic resonance

^{1}H NMR spectroscopy was carried out using a Bruker ARX400 spectrometer operating at 400 MHz and a temperature of 75 °C. Samples were prepared by dissolving the carrageenans in deuterium oxide (D_2O) at a concentration of 10 mg mL^{-1}. To quantify the biopolymeric fraction,

3-(trimethylsilyl)-L-propane sulfonic acid (Sigma-Aldrich, USA) served as the internal standard, following the methodology described in a previous study (Hilliou et al. 2006).

Chemical shifts were referenced to the κ-carrageenan signal at 5.09 ppm. Spectral assignments were made based on previously published data (Van De Velde et al. 2001; 2002; 2004). The molar fractions (% mol) of the different carrageenan types were calculated by dividing the integrated intensity of each relevant ^{1}H NMR peak by the total integrated intensity of all assigned carrageenan anomeric protons (Azevedo et al. 2013).

High-performance size-exclusion chromatography and molecular weight determination

The molecular weight profile of carrageenans was analyzed using high-performance size exclusion chromatography (HPSEC) implemented on a HPLC system (Agilent Technologies). Separation was achieved with a TSKGel Super-Multipore PW-H column (6 × 150 mm), along with a corresponding guard column (TSKGel SuperMP(PW)-H, 4.6 × 35 mm), both supplied by Tosoh Bioscience, Japan. Approximately 5–10 mg of the dried sample were weighed and dissolved in 1 mL of the mobile phase under gentle stirring at room temperature until fully dissolved. The solution was then filtered through a 0.45 µm syringe filter prior to injection into the column. An aqueous solution of 0.1 M Na_2SO_4 served as the mobile phase, maintained at a flow rate of 0.3 mL min^{-1}. The column temperature was kept steady at 55 °C throughout the run. A refractive index detector (RID) was used for monitoring the eluting compounds. Calibration of the system was conducted using polyethylene oxide standards (PEO, Tosoh Bioscience, Japan) with weight-average molecular weights ranging from 2.36 × 10^4 to 7.86 × 10^5 g mol^{-1}. Because the RID output is directly related to the mass concentration of the polymer at each elution time, the area under the RID signal for each slice (RID_i) corresponds to the mass of polymer present in that fraction. This allows for the estimation of the number of polymer molecules (N_i) in the i-th fraction using the following approach:

$$N_i = k \cdot \frac{RID_i}{M_i} \tag{1}$$

M_i denotes the molecular weight of the polymer fraction eluting during time slice i, while k represents a proportionality constant. Using this relationship, both the number-average molecular weight (M_n) and the weight-average molecular weight (M_w) can be derived. Notably, the constant k cancels out in the respective equations, allowing for direct computation of M_n and M_w based on the measured data.

$$M_n = \frac{\sum N_i M_i}{\sum Ni} = \frac{\sum \left(k \cdot \frac{RID_i}{M_i} \cdot M_i\right)}{\sum \left(k \cdot \frac{RID_i}{M_i}\right)} = \frac{\sum RID_i}{\sum \left(\frac{RID_i}{M_i}\right)} \tag{2}$$

$$M_w = \frac{\sum N_i M_i^2}{\sum N_i M_i} = \frac{\sum \left(k \cdot \frac{RID_i}{M_i} \cdot M_i^2\right)}{\sum \left(k \cdot \frac{RID_i}{M_i} \cdot M_i\right)} = \frac{\sum (RIDi \cdot Mi)}{\sum RID_i} \tag{3}$$

It should be noted that HPSEC distinguishes molecules according to their hydrodynamic volume in solution, rather than by their molecular weight alone. This volume shows a stronger correlation with the M_w than with the number-average M_n. As a result, calibrating the system using M_w values from standard polymers aligns more closely with the actual separation process, offering a more accurate depiction of polymer dimensions in solution.

Film and gel formulation and thermo-rheological assays

Films were prepared using a 3:1 carrageenan to polyethyleneglycol 600 (PEG600) ratio, where PEG600 was used as a plasticizer. This corresponded to 3% (w/v) carrageenan and 1% (w/v) PEG600 in 9 mL of solution (0.27 g carrageenan and 0.09 g PEG600). The mixture was heated and stirred at 60 °C for 15 min. Film formation was carried out by casting 2 mL of the solution into a circular plastic mold. Films were obtained after oven-drying at 50 °C for 24 h. Gels were formulated identically as films, but without PEG600 and without drying, and measured after stabilizing for 24 h at 4 °C.

The gels and films were analyzed using a MCR302 controlled-stress rheometer (Anton Paar) to evaluate their rheological properties. A sand blasted parallel plate (25 mm) was used as measuring system. Samples were placed between the plates (0.1 mm gap), rested for 5 min prior to the rheological testing. Small amplitude oscillatory measurements, in terms of elastic modulus (G'), viscous modulus (G'') and complex viscosity (η*) were run at 25 ºC and 15 Pa within the linear viscoelastic region (34 Pa). Note here that stress sweeps were previously made at 1 Hz to define the linear viscoelastic region (< 34 Pa). All measurements were made at least in duplicate.

Color properties

Color characteristics of the formulated films were evaluated in the CIEL*a*b* color space using the corresponding color coordinates:

L*(lightness ranging from 0 (black) to 100 (white);
a*varying from red (a* > 0) to green (a* < 0); and
b* ranging from yellow (b* > 0) to blue (b* < 0).

Measurements were carried out using a CR-400 colorimeter (Konica Minolta, Tokyo, Japan). All measurements were performed at least in ten replicates.

Statistical analysis and software

Multiple linear regression models and its graphical representations were carried out using Design-Expert software version 13.0 (Stat-Ease Inc., USA).

Results and discussion

Schematic procedure and extraction yields

To comprehensively evaluate different strategies for crude carrageenan (CCAR) extraction from *M. stellatus*, seven process pathways were designed, each targeting different biomass fractions and treatment combinations (Fig. 1). In general, yields are in the range of simmilar aqueous extraction procedures reported elsewhere (Blanco-Pascual et al. 2014; Flórez-Fernández et al. 2022; Qiu et al. 2022; Sarkar et al. 2022). The added novelty of the present study was the obtention of carrageenans from solid residues, in a second extraction step. Figure 2A depicts various materials which result through the extraction process.

The first set of pathways focused on the sequential valorization of biomass following a hydrothermal treatment conducted under previously optimized conditions at 130 °C (Flórez-Fernández et al. 2022). From the liquid phase of hydrothermal-assisted extraction, 11.1 ± 3.2% (mean ± SD) of CCAR-1 were obtained. The solid residue (SR) from this process was further subjected to two downstream treatments: the first one yielded 33.45 ± 3.09% of CCAR-2 through a combined enzymatic (Cellic® CTec3) and ultrasound treatment, whereas the second one produced 27.66 ± 3.23% of CCAR-3 by ultrasound alone, enabling assessment of mechanical disruption in the absence of enzymatic action.

A second group of pathways explored carrageenan extraction directly from ultrasound-pretreated biomass. In this case, 23.67 ± 2.20% of CCAR-4 were obtained following a 3-h ultrasound pretreatment, by shaking at 55 °C for 24 h. This shaking step served as a control extraction without enzymatic input, allowing comparison against enzyme-assisted strategy. Subsequently, 18.22 ± 2.69% of CCAR-5 were extracted from the solid residue via ultrasonication at 80 °C for 1 h.

To evaluate enzymatic hydrolysis independently of hydrothermal extraction, CCAR-6 was obtained (38.50 ± 4.71%) through a 24 h treatment with Cellic® CTec3. Finally, CCAR-7 extended this route by subjecting the residual solid from CCAR-6 to ultrasonication at 80 °C for 1 h, demonstrating that additional polysaccharides could still be extracted from the remaining biomass. The enzymatic treatment alone (CCAR-6) produced the highest yield (38.50 ± 4.71%), highlighting the effectiveness of targeted enzymatic hydrolysis in disrupting the structural polysaccharide matrix, allowing

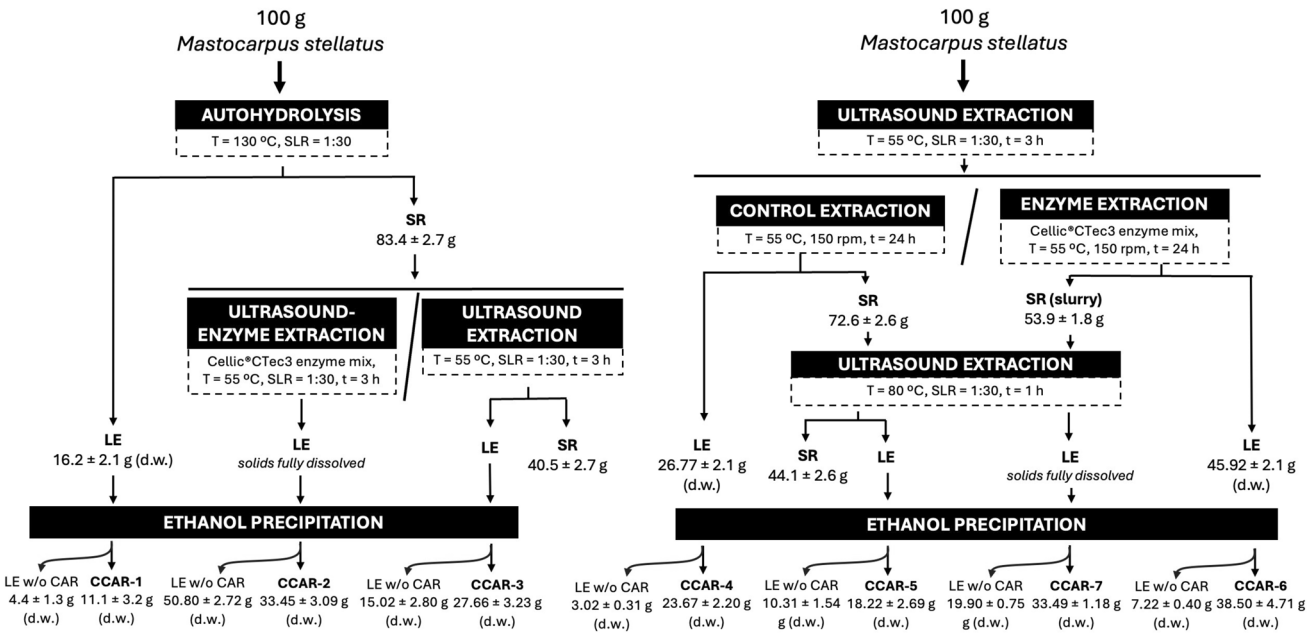


Fig. 1 Flowchart of sequential and alternative (/) processing pathways for crude carrageenan obtention. LE: Liquid extract; SR: Solid residue; CCAR: Crude carrageenan; LE w/o CAR: Liquid extract without carrageenan

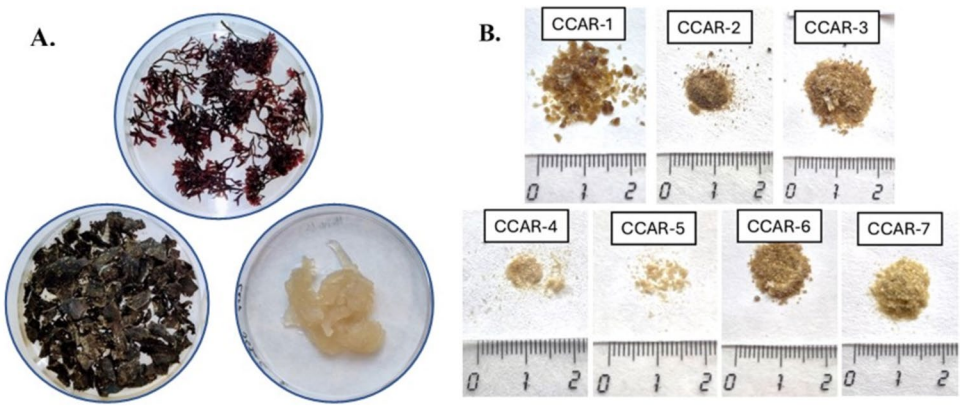


Fig. 2 Physical appearance of (**A**) *Mastocarpus stellatus* processing stages (top: *M. stellatus* gametophytic starting material, left: solid residue, right: ethanol-precipitated carrageenan before beeing dried) and (**B**) Obtained carrageenan powders from the different extraction pathways

deeper access to carrageenan that is otherwise embedded or tightly associated with the cell structure. The combination of enzymatic and ultrasound treatments in CCAR-2 also delivered a high yield (33.45 ± 3.09%), suggesting that physical disruption enhances enzyme accessibility and facilitates mass transfer. Ultrasound alone (CCAR-3), while slightly less effective (27.66 ± 3.23%), still significantly improved recovery compared to baseline methods, demonstrating the mechanical role of cavitation in disrupting cell walls and promoting carrageenan solubilization. The lower yield compared to CCAR-2 reflects the absence of enzymatic effects, indicating that mechanical energy alone cannot fully liberate polysaccharides from the biomass matrix.

In contrast, the hydrothermal extracted liquid fraction yielded relatively little carrageenan (CCAR-1, 11.1 ± 3.2%), while a significant fraction of carrageenan remained entrapped in the solid residue, as subsequent treatment of the SR still yields considerable carrageenan.

Interestingly, a previous study using the same macroalgal biomass reported a higher crude carrageenan yield at a SLR of 1:30, achieving 30.2% (Flórez-Fernández et al. 2022). Although the equipment used differed, resulting in variations in heating curves and process severity, the increased yield at lower SLR may be attributed to enhanced mass transfer efficiency and improved solvent penetration due to the greater volume of extracting medium.

Similarly, Torres et al. (2021), who obtained crude carrageenan yields of up to 40.3%, reported that the highest yields were obtained at an SLR of approximately 2.09 g per 100 g (equivalent to 1:48), with yields decreasing at both lower and higher SLRs. This suggests the existence of an optimal solvent volume for maximizing carrageenan release. In our study, however, a considerable amount of carrageenan remained adsorbed to the solid residue, indicating incomplete extraction and highlighting the need to optimize conditions further.

Nevertheless, despite the comparatively lower yield, an SLR of 1:20 may represent a more energy-efficient and economically viable extraction condition, as it involves heating a smaller liquid volume, thus reducing both energy consumption and liquid waste generation. However, in the case of ultrasound-assisted extraction, lower SLRs (i.e., lower solid concentrations) are often necessary to reduce viscosity-related limitations that can impair ultrasonic wave propagation and cavitation efficiency (Meroni et al. 2022). This justifies the use of lower concentration conditions such as an SLR of 1:30 when ultrasonication is applied.

Pathways CCAR-4 and CCAR-5, included a shaking step as a control extraction, after a US pretreatment (23.67 ± 2.20%) and a follow-up ultrasound treatment of the SR (18.22 ± 2.69%). The shaking step simulates prolonged soaking under moderate thermal conditions and demonstrates that a notable fraction of carrageenan can be extracted without enzyme assistance. However, its yield is lower than that of enzyme-assisted strategies, reinforcing the added value of enzymatic catalysis. The fact that the SR from this process still yielded a significant amount of carrageenan after ultrasound (CCAR-5) underscores the incomplete extraction during the control extraction, possibly due to the presence of more tightly bound polysaccharides requiring further matrix disruption. Simmilarly, applying ultrasound to the residue remaining after enzymatic extraction, recovered additional carrageenan (CCAR-7). This indicates that even enzymatic treatment does not exhaust all available carrageenan, due to substrate inaccessibility or incomplete digestion. The capacity of ultrasound to further disrupt the biomass and liberate residual carrageenan highlights the complementary roles of enzymatic and mechanical treatments.

Although direct comparisons are difficult due to differences in the purity of recovered carrageenans and the natural variability of the starting biomass, conventional alkali-based extractions typically yield between 25–50%. For instance, Azevedo et al. (2013) reported 30–43% and 40–50% yields after 3% w/v KOH and NaOH pretreatments, respectively, while Hilliou et al. (2006) obtained around 25% using a milder 0.1 M Na_2CO_3 pretreatment.

Liquid extracts remaining after sulfated polysaccharide precipitation, obtained from cellulase/hemicellulase digestion of seaweed or its solid residue, contain high amounts of glucose as reported by Baltrusch et al. (2024) in a similar study using *Ulva* spp. (Chlorophyta) as raw material and the same enzyme mix. These streams may have potential for valorization as byproducts. However, this statement is based on logical inference rather than direct measurement in the present study. Further research is necessary to evaluate the exact composition of the byproducts and their practical applications. Still, our findings may contribute to a sequential or combinatory approach for crude carrageenan recovery and for process intensification strategies in seaweed biorefinery.

Life-cycle and process analyses of cellulase production, along with Novozymes' published data and sustainability reports, indicate that although the manufacture is relatively clean, avoiding the use of heavy or toxic reagents, it remains energy- and water-intensive, requiring approximately 69 MJ kg^{-1} (Olofsson et al. 2017) and 33 L kg^{-1} (Ellilä et al. 2017), respectively. The process also generates considerable amounts of organic waste (Olofsson et al. 2015), although Novozymes claims that these residues are industrially used for biogas generation (Ørsted 2017). These values, however, can vary depending on specific production conditions. While enzymes are applied in relatively low quantities and therefore have a limited overall contribution to environmental impact, such factors should be considered in future life-cycle assessments of enzyme-assisted extraction products. This evaluation was beyond the scope of the present study but remains essential for a comprehensive assessment of the sustainability of this method.

In addition, it should be noted that EU organic regulations prohibit the use of genetically modified organisms (GMOs) or products derived from GMOs in organic food production. Since many commercial cellulase preparations, including Cellic® CTec3 (U.S. Food and Drug Administration 2020), are produced using genetically modified production strains, their use as processing aids in enzyme-assisted extraction would not currently be compatible with EU organic certification of carrageenan production.

Chemical structure of carrageenan

Extracted polysaccharides were qualitatively assesed using FT-IR spectroscopy. Figure 3 shows FT-IR profiles of the crude carrageenans extracted through different processes, described in the previous section. The spectra exhibited the typical ι-band (at 805 cm^{-1}) and a stronger κ-band (at 845 cm^{-1}), corresponding to 3,6-anhydro-galactose-2-sulphate and galactose-4-sulphate, respectively. The absorption band at 930 cm^{-1} suggests symmetric stretching of the (C-O-C) anhidro group, which can be attributed to the presence of

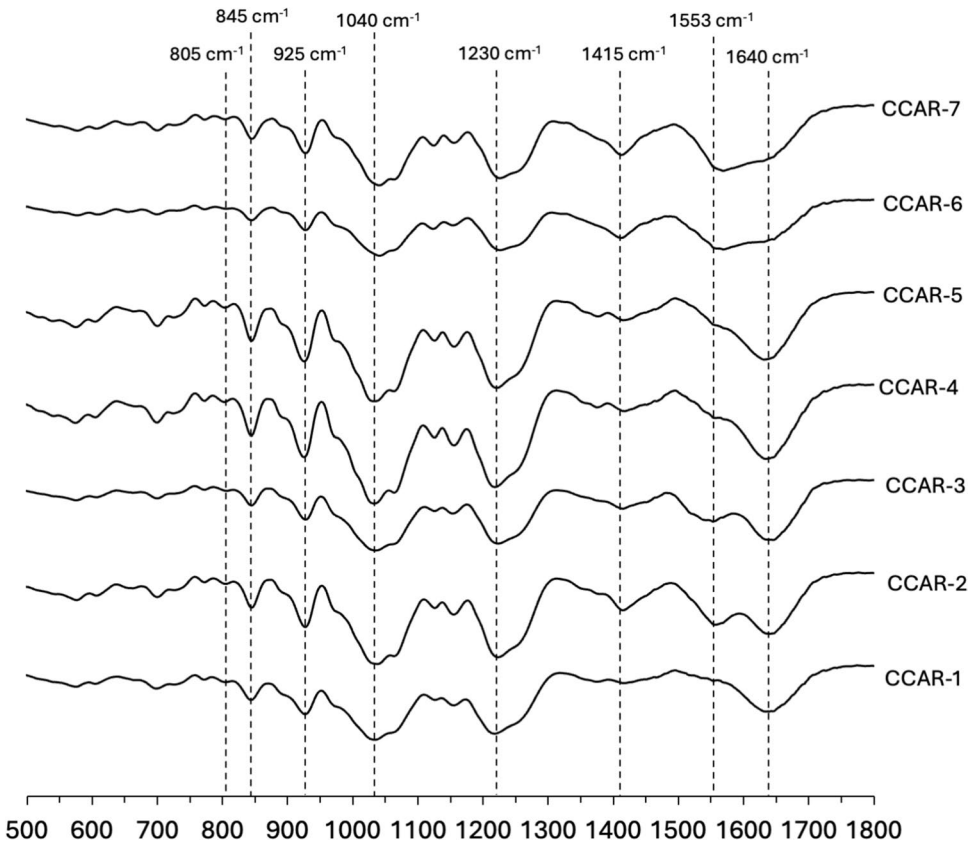


Fig. 3 Fourier transform infrared spectra of crude carrageenans (CCAR) after different extraction procedures from *Mastocarpus stellatus*. CCAR-1: Hydrothermal-assisted extraction (T = 130 ℃). CCAR-2: US-assisted extraction from CCAR-1 pathway solid residue. CCAR-3: US plus enzyme-assisted extraction of carrageenan from CCAR-1 pathway solid residue. CCAR-4: US-assisted extraction followed by warm-water extraction with shaking. CCAR-5: US-assisted extraction from the solid residue of the CCAR-4 pathway. CCAR-6: US-assisted extraction followed by enzymatic digestion. CCAR-7: Ultrasound-assisted extraction from the solid residue of the CCAR-6 pathway

3,6-anhydro-galactose. Another typical broad absorption band around 1230 cm^{-1} corresponds to the esther sulphate groups (S=O stretching). These results are consistent with (hybrid-)carrageenan characterizations in other studies (Prado-Fernández et al. 2003; Pereira et al. 2009; Pereira and Van De Velde 2011; Huang et al. 2024). The different extraction procedures showed little difference, only at 1553 cm^{-1} SR-derived carrageenans showed a stronger absorption. The intensity ratio between the 805 and 845 cm^{-1} peak absorption bands, can be used to qualitatively determine the degree of ι/κ hybridization (Pereira et al. 2009; Azevedo et al. 2022). This ratio gave hybridization values of 0.32 for CCAR-1, 0.21 for CCAR-2, 0.29 for CCAR-3, 0.20 for CCAR-4, 0.10 for CCAR-5, 0.36 for CCAR-6, and 0.24 for CCAR-7. This suggests a predominance of κ-carrageenan in all samples.

The relation of sulfate to total carbohydrate was estimated from the ratio between absorbances at 845 and 2920 cm^{-1}, as described by (Rochas et al. 1986). This ratio was expressed as a degree of sulfation (DS), representing the average number of sulfate groups (in moles) per disaccharide repeat unit within the carrageenan structure. In this method, the 845 cm^{-1} band corresponds to sulfate ester vibrations, while the 2920 cm^{-1} band serves as a reference for the polysaccharide backbone (C-H stretching). Although it provides only an approximate measure of the DS, it offers a useful comparative indicator among samples. DS ≈ 1 is typically associated with κ-carrageenan predominance. The estimated DS values were 0.85 for CCAR-1, 0.81 for CCAR-2, 0.65 for CCAR-3, 0.83 for CCAR-4, 0.89 for CCAR-5, 0.68 for CCAR-6, and 0.72 for CCAR-7. These results <1, indicate either partial desulfation or presence of polysaccharide contamination (e.g., floridean starch) because of the predominance of the C-H stretching**.**

As representative examples, ^{1}H NMR spectra of CCAR-1,2, and 3, were included in Figure 4. The location and strength of the anomeric signals in the ^{1}H NMR spectrum (within the range of 5.0–5.6.0.6 ppm) provides a representation of the monomeric composition of carrageenan, including both the types of repeating units and their respective relative quantities (Van De Velde et al. 2001; Hilliou et al. 2006). Peaks corresponding to hidrogens of anomeric carbons were tentatively characterized, attending to data found in literature, as summarized in Table 1, and pointed out by vertical arrows in Fig. 4. The hybrid carrageenan preparations from *M. stellatus* resulted to be made of κ-, ι-, ν-, and μ-carrageenan, in line with previous studies (Azevedo et al. 2022). Peaks at 5.28 and 5.09 ppm revealed the presence of ι- and κ-monomers. The minor peak at 5.50 ppm, present in all samples, can be assigned to the anomeric proton of ν-monomers. A slight shoulder at 5.22 ppm, which becomes more pronounced in the CCAR-2 sample, might be indicative of μ-carrageenan. This particular carrageenan variant was previously identified at 5.238 ppm by Van De Velde et al. (2004); however, the subtle differences in the chemical shift pose some ambiguity. A signal at 5.13 ppm was also observed within the anomeric region of the spectra of CCAR-1, and as a shoulder in CCAR-3. To the best of the authors knowledge, no similar peaks have been discussed in the literature, although also present in carrageenan samples of *M. stellatus* analyzed by Azevedo et al. (2022). Despite the precise origin of this signal cannot be confirmed, we tentatively hypothesize that it may be associated with the α-anomeric proton of κ-monomers, which typically resonates near 5.09 ppm, but appears slightly downfield in our samples. This interpretation is speculative and may reflect subtle variations in the local chemical environment, such as differences in counterion composition, hydrogen bonding, or molecular packing; resulting in a subpopulation of κ-type units located in distinct microenvironments (e.g., chain termini, branch points, or regions with variable sulfation), rather than the presence of a different carrageenan monomer.

Floridean starch, a branched (1→4,1→6)-α-D-glucan with structural similarities to plant amylopectins and animal glycogens, serves as a storage polysaccharide in red algae. It exhibits solubility in water and can be found alongside carrageenans during extraction and precipitation processes (Van De Velde et al. 2002). In the ^{1}H NMR spectra, the presence of floridean starch is indicated by the signal corresponding to the anomeric proton of the α-(1→4)-linked D-glucopyranosyl moiety, which was assigned to the 5.39 ppm peak, of negligible intensity, simmilarly to the peak 5.38 ppm reported by Azevedo et al. (2022) who analyzed carrageenans from *M. stellatus*, and relatively next to the peak at 5.35 ppm reported in literature (Van De Velde et al. 2002; Pereira and Van De Velde 2011). On the other hand, pyruvic acid, which is a common subsituent of complex carrageenans (Van De Velde et al. 2004), could not be identified.

The ^{1}H NMR spectrum provides evidence crude carrageenans extracted from *M. stellatus* are primarily composed of κ- and ι-monomers, with minor traces (above 5% relative content, considering the NMR spectroscopy detection limit) of μ- and ν-monomers (Table 1). As a result, these biopolymers can be described as κ/ι-hybrid carrageenans, indicating the presence of both κ- and ι-monomers within the same macromolecule (Hilliou et al. 2006). CCAR-2 showed an interestingly high amount of μ-carrageenan, suggesting that the enzymatic extraction could facilitate the liberation of this carrageenan from the cell-wall matrix.

Analysis of obtained samples revealed that CCAR-1 consists of 58.14 mol% κ-, 29.07 mol% ι-, 6.98 mol% ν- and 5.81 mol% μ-carrageenan. These findings are in reasonable agreement with results reported by Pereira & Van De Velde (2011) or Hilliou et al. (2006) for *M. stellatus* carrageenan. CCAR-2 and specially CCAR-3 carrageenans showed an increased ν-carrageenan mol%, showing that it

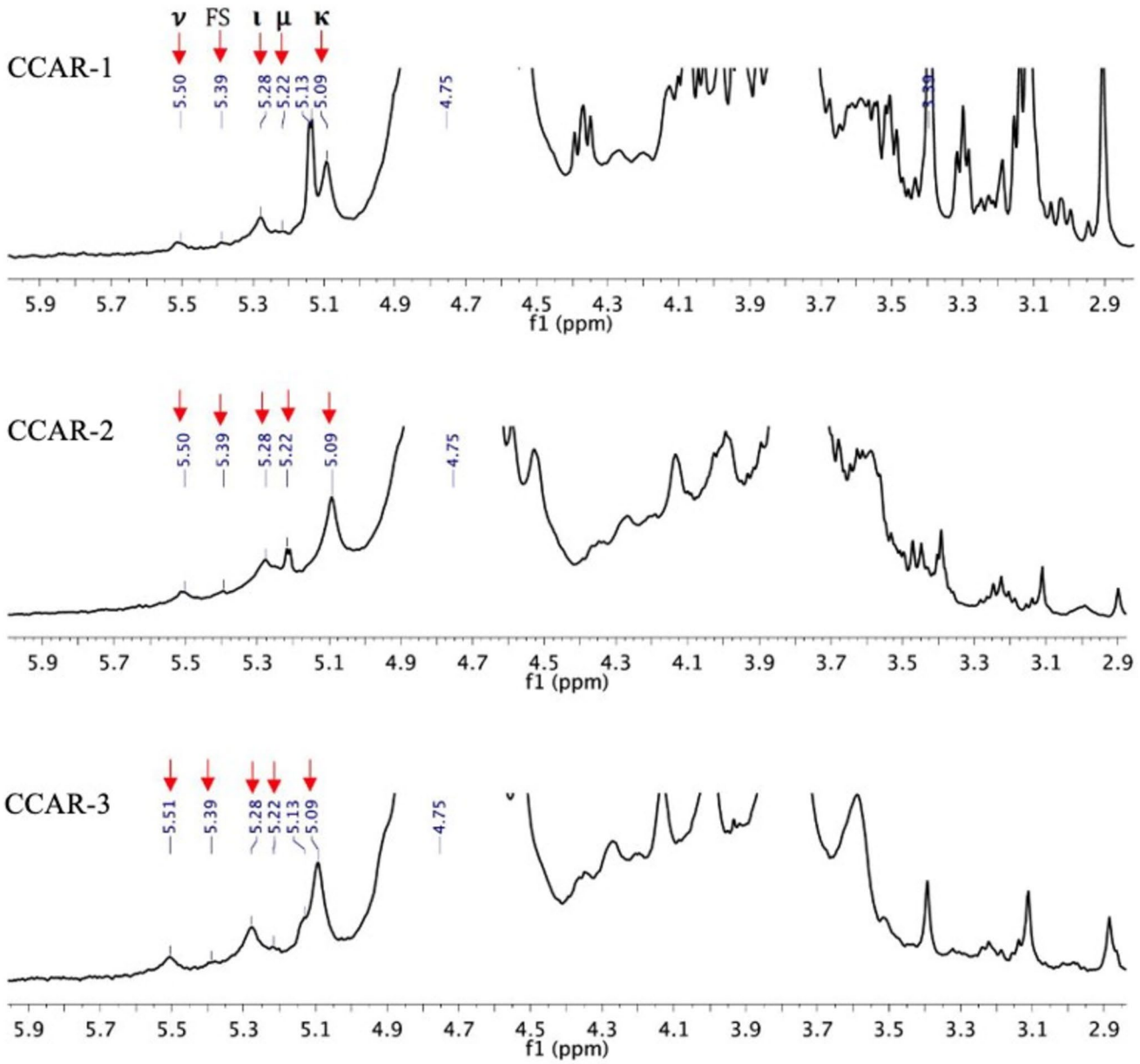


Fig. 4 ^{1}H NMR spectra of representative examples of crude carrageenans extracted from *Mastocarpus stellatus*. CCAR-1: Hydrothermal-assisted extraction (T = 130 ºC). CCAR-2: US-assisted extraction from CCAR-1 pathway solid residue. CCAR-3: US plus enzyme-assisted extraction of carrageenan from CCAR-1 pathway solid residue. Relevant peaks are pointed out with arrows and show floridean starch (FS) and signals of hydrogens from anomeric carbons

Table 1 Representative examples of crude carrageenan composition obtained by ^{1}H-NMR spectroscopy

Carrageenan forms	Repeating unit composition (mol%)		
	CCAR-1	CCAR-2	CCAR-3
ι (iota)	29.07	28.43	29.79
κ (kappa)	58.14	49.02	53.19
λ (lambda)	0	0	0
ν (nu)	6.98	9.31	11.17
μ (mu)	5.81	13.24	5.85

is possible to obtain these polysaccharides from the SR through a second extraction step.

Obtaining the ν- and μ-carrageenan content from the ^{1}H NMR spectra proved difficult due to the small corresponding signal (except in case of μ-carrageenan in CCAR-2), showing up as a shoulder alongside the peak assigned to ι-carrageenan. This overlap maked it challenging to perform accurate quantitative analyses; thus, results should be taken with care.

As pointed out by Azevedo et al. (2022), the elevated molecular weight of these carrageenan samples may account for the reduced resolution observed in the respective ^{1}H NMR spectra, which, in turn, could potentially influence the quantification results presented in this study, which intend to be representative, indicative measures rather than exact quantifications.

Proximate composition and molecular weights of crude carrageenans

To evaluate the quality and structural characteristics of crude carrageenan fractions obtained through various extraction strategies from *M. stellatus*, proximate composition and molecular weights were analyzed (Table 2). Additionally, molecular weight profiles are represented in Fig. 5. These data offer essential insights into both the efficiency and selectivity of each process route.

While the use of PEO standards and the derived Eqs. (2) and (3) for M_n and M_w are valid for determining the "relative" molecular weight distribution, it is important to recognize that carrageenans differ structurally and conformationally from PEO. Carrageenans are semi-rigid, highly sulfated polysaccharides, whereas PEO is a flexible, neutral polymer. As HPSEC separates based on hydrodynamic volume rather than absolute molecular mass, the calibration curve generated using PEO standards may not precisely reflect the elution behavior of carrageenan molecules and likely causes a slight overestimation of molecular weights. Consequently, the molecular weights reported here should be interpreted as "apparent" or "relative" to PEO callibration and may differ from absolute values obtained through methods such as multi-angle light scattering (MALS) or intrinsic viscosity measurements.

Ash content varied significantly across carrageenan samples, reflecting differences in co-extracted inorganic matter among treatments. Lowest value was observed for CCAR-1 (17.02 ± 1.56%) and CCAR-4 (20.52 ± 1.48%), corresponding respectively to the hydrothermal extraction and an ultrasound extraction followed by warm-water shaking. These relatively low ash contents suggest cleaner extractions due to reduced structural disruption and limited release of mineral-bound compounds. In contrast, enzymatically extracted carrageenans exhibitted high ash contents, which peaked in CCAR-7 (35.54 ± 2.07%). Moreover, carrageenans from solid residues had higher ash contents than from initial extractions. Ash contents are indicated as mean ± SD and were calculated from n = 3 independent samples.

Protein content also showed notable differences across samples, with values ranging from 6.11 ± 0.14% (CCAR-7) to 14.40 ± 0.47% (CCAR-2); mean ± SD, n = 3. Treatments involving enzymatic hydrolysis, such as CCAR-2 and CCAR-6, tended to yield carrageenan with higher protein content, likely due to the liberation of proteins of the cell-wall or protein-polysaccharide complexes during cell wall degradation. A similar tendency regarding protein contamination was observed in a prior study with the same enzyme mix applied on ulvan extraction (Baltrusch et al. 2024). Conversely, CCAR-7, which followed enzymatic treatment with additional ultrasound, demonstrated the lowest protein content.

M_w is a critical indicator of carrageenan functionality, influencing rheological behavior, gel strength, and solubility. The highest M_w was observed in the control commercial sample (CC: 1530.73 ± 27.23 kDa), followed by CCAR-4 (1373.13 ± 2.24 kDa) and CCAR-5 (1418.75 ± 20.42 kDa). In contrast, CCAR-2 (530.22 ± 6.69 kDa) and CCAR-3 (453.86 ± 10.82 kDa) exhibited significantly lower M_w values. Notably, CCAR-6 (enzymatic assisted extraction) preserved a relatively high M_w (1210.79 ± 21.01 kDa), highlighting the capacity of enzymatic hydrolysis to extract carrageenan efficiently while maintaining structural integrity. M_w results are provided as mean ± SD, n = 3.

The overall lower M_n and M_w molecular weights observed in carrageenan fractions obtained downstream of hydrothermal extraction (CCAR-1 to CCAR-3) compared to those from alternative extraction pathways (CCAR-4 to CCAR-7) can be attributed to the conditions of subcritical water treatment. Hydrothermal extraction, conducted at elevated temperature (130 °C), likely initiates partial thermal depolymerization, although not necessarily improving the cell wall matrix disruption compared to US and enzymatic

Table 2 Proximate composition and apparent molecular weights of obtained crude carrageenans (CCAR) and commercial carrageenan (CC); results are shown as mean ± SD, n = 3

	CC	CCAR-1	CCAR-2	CCAR-3	CCAR-4	CCAR-5	CCAR-6	CCAR-7
Ash	18.35 ± 1.15	17.02 ± 1.56	20.74 ± 1.31	33.01 ± 1.74	20.52 ± 1.48	21.90 ± 1.43	25.90 ± 1.52	35.54 ± 2.07
Protein	2.85 ± 0.15	9.84 ± 1.93	14.40 ± 0.47	7.38 ± 0.26	6.93 ± 0.24	8.64 ± 0.36	11.03 ± 0.55	6.11 ± 0.14
Mw (kDa)	1530.73 ± 27.23	1087.48 ± 18.15	530.22 ± 6.69	453.86 ± 10.82	1373.13 ± 2.24	1418.75 ± 20.42	1210.79 ± 21.01	1176.32 ± 22.20
Mn (kDa)	251.38 ± 4.00	331.87 ± 2.76	190.56 ± 2.25	179.23 ± 2.45	382.57 ± 17.94	378 ± 15.31	350.62 ± 7.34	384.56 ± 35.10
PDI	5.54 ± 0.76	3.13 ± 0.18	2.89 ± 0.15	2.56 ± 0.06	3.59 ± 0.16	4.3 ± 0.97	3.45 ± 0.13	3.07 ± 0.22

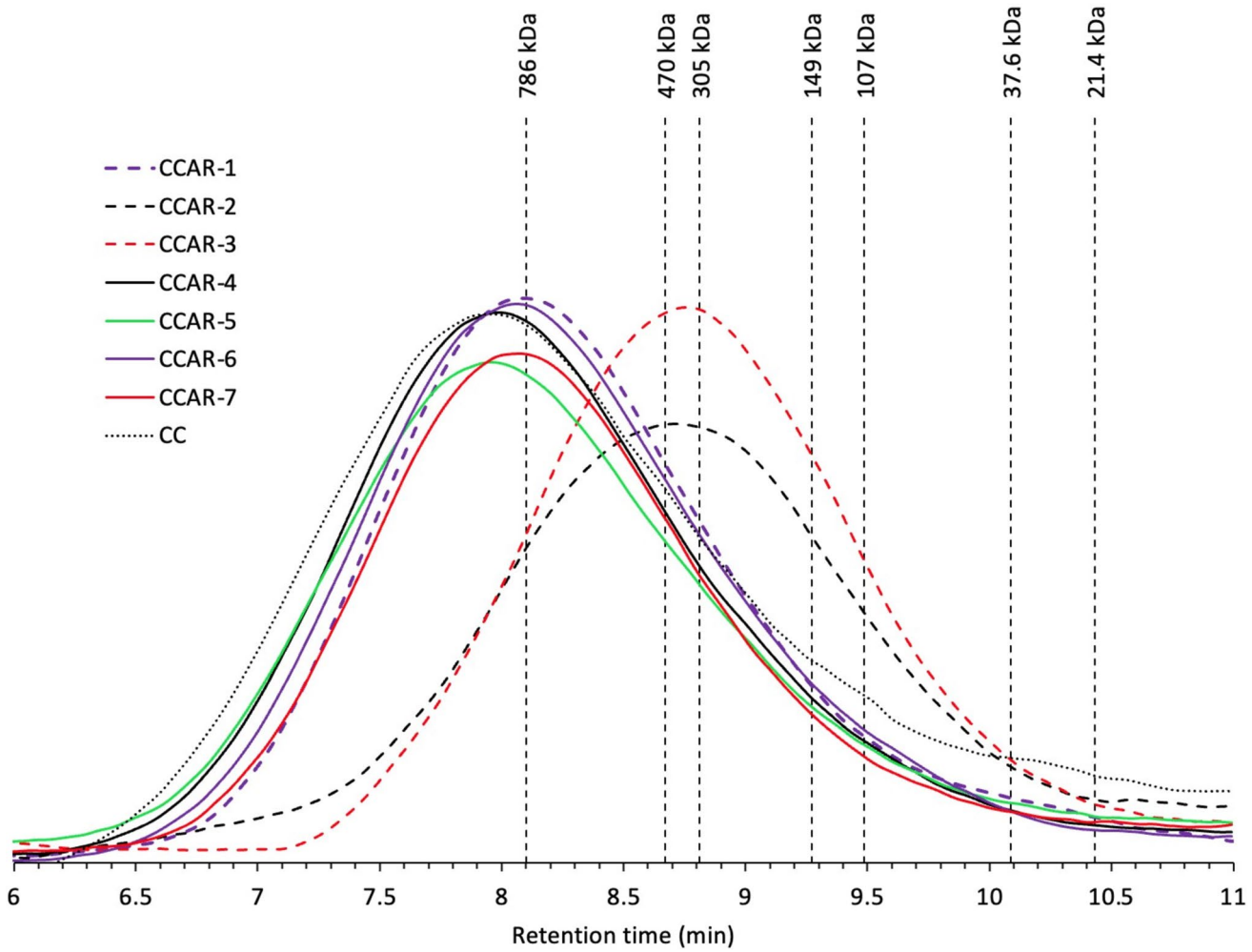


Fig. 5 HPSEC profiles of obtained carrageenans, and commercial carrageenan (CC)

extractions. In fact, results suggest a preferential recovery of larger molecular weight fractions during hydrothermal extraction step (although thermal depolymerization may involved), followed by liberation of smaller fractions, more entangled or deeper embedded within the cell-wall matrix, in downstream processes, when ultrasonication or enzymatic digestion is performed over the solid residues. This is evidenced by the contrast between CCAR-1 (M_w: 1087.48 kDa) and the subsequent fractions CCAR-2 and CCAR-3 (M_w: 530.22 and 453.86 kDa, respectively), which were extracted from the solid residue by ultrasonication, with or without enzymatic input, facilitating its release.

In a similar tendency, when comparing CCAR-4,5 and CCAR-6,7, slighly lower M_w are observed in enzymatically extracted carrageenans (1373.13 and 1418.75 kDa *vs.* 1210.79 and 1176.32 kDa) Although enzymatic treatment (CCAR-6) did not involve depolymerizing conditions per se for carrageenan, it probably caused the greater liberation of more deeply embedded or matrix-bound smaller carrageenan chains, due to the enzymatic disruption of the cell wall. Thus, the observed M_w reduction in ultrasound, and enzymatic treatments, is the result of a more pronounced extraction or a stronger and complemental disruption of structurally different, more entangled, more embedded carrageenan fractions.

Notably, CCAR-4 and CCAR-5 displayed comparable M_w and M_n values (M_w: 1373.13 and 1418.75 kDa; M_n: 382.57 and 378.00 kDa, respectively), consistent with the similarity in treatment severity between these two protocols; both relying on mechanical agitation and ultrasound without enzymatic digestion. Likewise, the close molecular weight values between CCAR-6 and CCAR-7 (M_w: 1210.79 and 1176.32 kDa) suggest that the post-enzymatic ultrasound treatment in CCAR-7 did not cause significant further extraction of smaller carrageenan fractions, likely because it only prolonged the extraction of similar fractions from an already predigested matrix.

Interestingly, M_n values across CCAR-4 to CCAR-7 remained relatively stable, ranging from 350.62 to 384.56 kDa, indicating that the most common chain size within each extract was not significantly altered by variations in treatment. This stability in M_n suggests that although M_w and polydispersity index (PDI) were affected by process conditions, the dominant carrageenan fraction consistently resided within a similar size range. Such findings imply that treatment severity influences chain length distribution and extract uniformity more than the modal size of carrageenan polymers.

Film formulation, colour and rheological analyis

The morphology of carrageenan films is influenced by factors such as carrageenan type, concentration, film formation method, and additives. Typically, these films show a smooth, uniform surface. However, adding substances like plasticizers or antimicrobial agents can cause rough, cracked, or non-uniform textures due to issues like nanoparticle aggregation or insoluble components (Sabu Mathew et al. 2024). These negative characteristics were not observed in the formulated films of the present study (F-1 to 7, formulated with CCAR-1 to 7, respectively), which only included PEG600 as plastisizer.

Colour analysis results are displayed in Table 3 and can be visually appreciated in Fig. 6C. The color properties of formulated films varied in a similar range for F-1 to 3, showing similar a* and b* values (although L* for F-3 was slightly higher), and F-4 to F-5 displaying comparable color coordinates. These variations reflect the influence of the different extraction conditions. Films formulated with carrageenans from hydrothermal extraction pathways (F-1 to 3) resulted in yellowish-brown-red color, with strong warm tone, and F-3 showing a lighter tone. In contrast, films formulated with carrageenans from ultrasonication extraction pathways, F-4 to 7, showed light yellowish color with minimal red tint, whith F-4 showing the lightest tone, with a very pale color.

The rheological properties of carrageenan films from different extraction methods reveal a detailed picture of how extraction strategies influence the resulting material characteristics in terms of storage modulus (G') and loss modulus (G"), as shown in Fig. 6A. The storage modulus (G') indicates the material elasticity, while the loss modulus (G") measures its viscous behavior.

Films derived from CCAR-1 (F-1), obtained from hydrothermal extraction, consistently demonstrated the highest G' across the frequency range, indicating a robust, elastic material. This behavior correlates with the higher compositional purity of the carrageenan (lowest ash and protein contents, 17% and 9%, respectively). Although other factors such as molecular weight and carrageenan structure may also influence the viscoelastic behavior, the observed trends suggest that reduced impurity levels contribute to improved film integrity. The second lowest ash+protein contents (20.5 and 6.93%, respectively), were measured for CCAR-4 which resulted in highest complex viscosity values in F-4, and second highest storage modulus measured. F-6 showed simmilar results, as CCAR-6 had a simmilar (although more contaminated) composition. The higher G' values in the latter sample also indicate that the carrageenan in these films has a more organized structure, likely due to the targeted enzymatic hydrolysis that extracts carrageenan with minimal degradation, which is coherent with the high M_w observed in this sample (1373 kDa, respectively). On the other hand, F-2, F-3 and specially F-7, showed the lowest complex viscosity and G'/G" values, which is in coherence with the low M_w observed for CCAR-2 and CCAR-3 (530 and 454 kDa, respectively) and the very high ash content in CCAR-7 (35.5 %).

In Fig. 6B, complex viscosity of gels, formulated without the addition of any other compouns, is shown. The ultrasound-control extraction in warm water produced the best crude carrageenan (CCAR-4) for gel formulation. Highest complex viscosities were obtained for G-4, G-5 and G-1, and lowest complex viscosities were obtained for G-7, G-6, G-2, and G-3 showing the influence off both the high ash content (negative effect) and Mw (positively affects complex viscosity).

In Fig. 7, multiple linear regression models were fitted to illustrate the main trends observed within the experimental region for the loss factor (tan δ = G'/G"), storage modulus (G'), and complex viscosity, in relation to the ash and protein content of the extracted carrageenans used to formulate the films. The purpose of these models was not to develop predictive tools, but rather to highlight general tendencies within the data. While the models did not reach conventional significance, the observed trend may still be meaningful, particularly given the limited sample size and consistent directional effect observed across replicates. No tendencies regarding effect of M_w could be identified as poor dataset on M_w variability.

Table 3 Color parameters (L*, a*, b*) of analyzed films (mean ± SD, n = 3, technical replicates)

	L*	a*	b*
F-1	65.02 ± 1.33	9.38 ± 0.97	39.75 ± 1.14
F-2	67.79 ± 1.40	9.22 ± 1.00	36.52 ± 1.02
F-3	86.5 ± 1.49	8.91 ± 0.84	33.45 ± 1.09
F-4	92.24 ± 1.02	−0.41 ± 0.63	14.01 ± 1.18
F-5	84.99 ± 1.26	−2.96 ± 0.81	32.56 ± 1.11
F-6	87.45 ± 1.35	−0.59 ± 0.85	28.16 ± 1.05
F-7	85.52 ± 1.21	−1.96 ± 0.80	30.06 ± 0.95

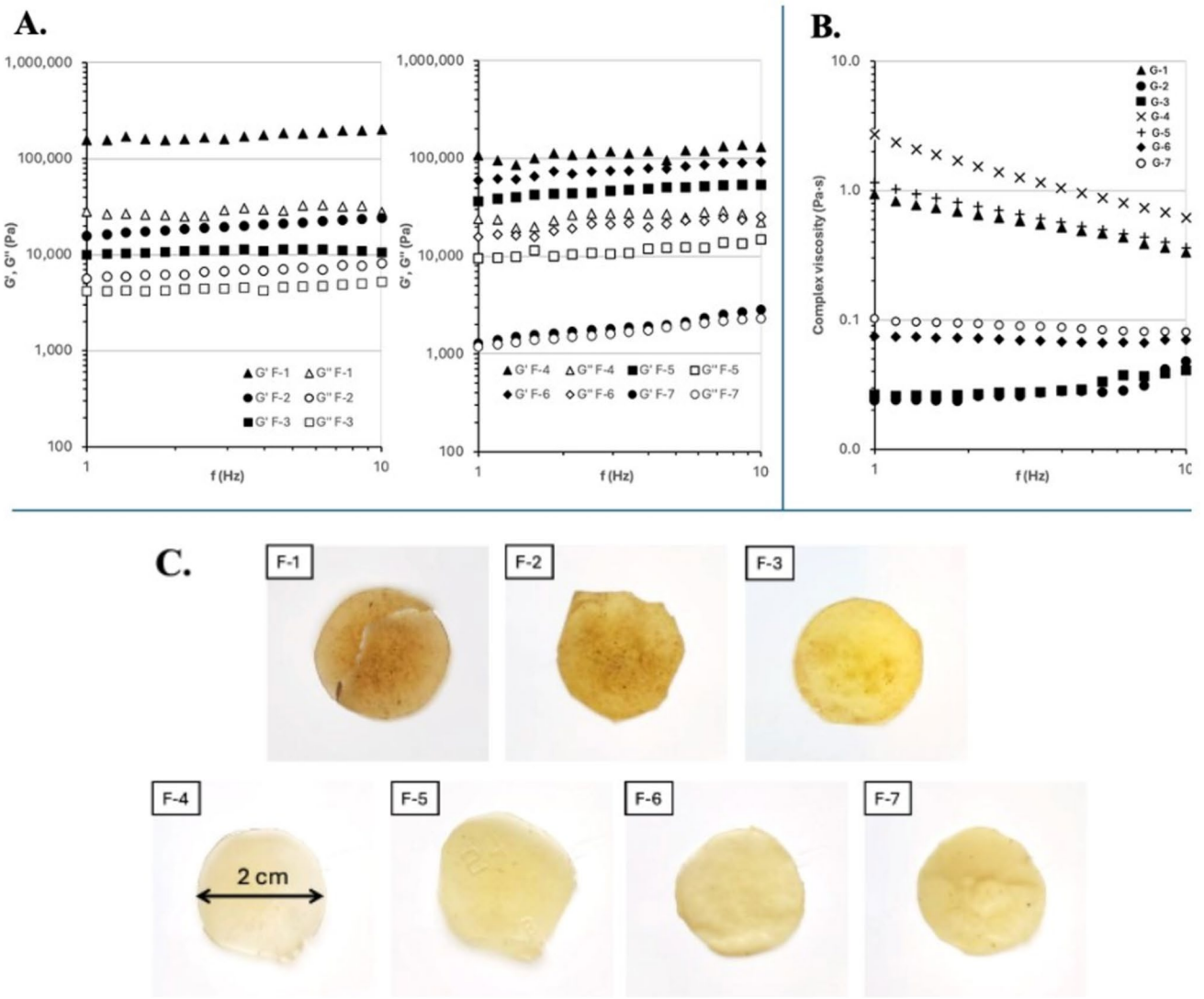


Fig. 6 A. Rheology of films formulated with different types of crude carrageenan. **B**. Rheology of formulated gels. **C**. Visual appearance of analyzed films (F), codes 1–7 correspond to type of carrageenan used in formulation (CCAR1-7). The film diameter represented in F-4 is representative of all films

A square root transformation was applied to the storage modulus (G′) and complex viscosity response variables to ensure non-negative predictions and stabilize variance. As a result, regions where the original model would have predicted negative values are not shown, since the square root of a negative number is undefined. This does not affect the interpretation of the main trends within the experimental region, which remain clearly visible and valid.

The coefficients of determination (R^2) and adjusted R^2 values were 0.69 and 0.54 for the loss factor, 0.81 and 0.61 for the storage modulus, and 0.76 and 0.64 for complex viscosity, respectively. These values indicate moderate to strong relationships, suggesting that ash and protein content contribute meaningfully to the variation observed in rheological properties. Protein content did not influence at all the loss factor (Fig. 7A), possibly because it either lacks structural impact in this system or contributes similarly to both G′ and G″, leaving their ratio (tan δ) largely unaffected. However, while statistical analysis showed that ash content had a signifficant effect in the model, contributions of protein content to the response variables were not stricktly signifficant (results not shown). In contrast, in a study performed by Blanco-Pascual et al. (2014), the incorporation of protein-rich hydrolysates into carrageenan-based films showed an significantly enhancement their functional properties. Increased protein content promoted stronger intermolecular interactions, such as hydrogen bonding, which improved film structure, reduced water vapor permeability, and enhanced flexibility and mechanical resistance. However, in this study, higher ash and protein content reduced the proportion of

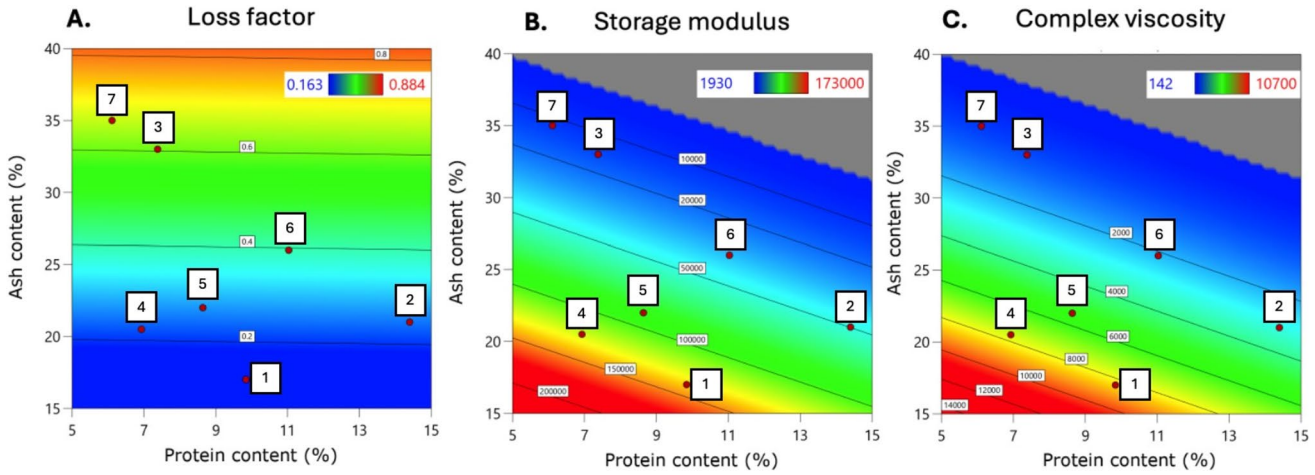


Fig. 7 Linear models showing the effect of ash and protein content on (**A**) the loss factor (tan δ), (**B**) storage modulus (G′), and (**C**) complex viscosity of carrageenans used in film formulations. Numbers 1–7 refer to the crude carrageenans (CCAR-1 to 7)

functional biopolymer per gram of crude carrageenan extract used in the film formulations, which may have affected the rheological properties of the resulting mixtures and lowered overall film stability. This is supported by the results in Fig. 7B, where lower ash and protein contents were associated with a tendency of higher storage moduli, and in Fig. 7C, with higher complex viscosity values. No clear trend in the effect of M_w was identified due to the limited variability in the dataset (results not shown).

Conclusions

In conclusion, hydrothermal extraction is an effective method for recovering high-quality crude carrageenans, although the recovery is lower compared to combined enzyme-ultrasound treatments with Cellic® CTec3 enzyme mix, which produce slightly lower-quality extracts for film-forming purpose but had better gelling behaviour. Ultrasound treatment enhances physical breakdown and mass transfer, particularly when combined with enzymes.

Carrageenans recovered from solid residues exhibited distinct properties, including lower molecular weight in the case of hydrothermal extraction-derived residues and increased ash content. Enzyme-US-extracted carrageenans showed higher ash content than those extracted using US alone, while both had greater ash content than carrageenans obtained via hydrothermal extraction. Shaking at 55 °C for 24 h demonstrated limited access to structurally bound carrageenan. Residual solids retain extractable carrageenan due to the complexity of the biomass matrix, indicating potential for multi-stage valorization.

Results show that higher molecular weights are released more easily and lower molecular weights after post-treatments of solid residues. Ash and protein contents correlate with rheological properties of formulated films and gels. The rheological analysis of the films highlights the critical role of extraction methods in determining the mechanical properties of carrageenan-based films as it influences M_w, protein content and ash content.

These findings contribute to the development of sustainable and viable carrageenan extraction protocols from red macroalgae and its extraction residues, which could contribute to integrated seaweed biorefineries and circular economy.

Future research should integrate techno-economic assessments, life cycle analyses, and carbon footprint evaluations to better determine the industrial and environmental feasibility of green carrageenan extraction processes as outlined in this study. Moreover, advances in the cultivation of red seaweeds such as *Mastocarpus*, will be crucial to support sustainable production and the development of biorefinery strategies for high-value applications. Future studies could focus on a more detailed characterization of the monosaccharide composition of liquid by-products following carrageenan separation, as well as on the structural and compositional analysis of the carrageenans themselves and the development of sustainable downstream purification methods.

Acknowledgements Authors acknowledge FTIR and NMR measurements to the services of analysis of Universidade de Vigo (CACTI).

Authors thank the financial support to the Ministry of Science, Innovation and Universities of Spain (RTI2018-096376-B-I00). M.D.T. acknowledges to the Ministry of Science, Innovation and Universities for the project (CNS2024-154456). K.L.B. acknowledges to the predoctoral fellowship program of the Ministry of Science, Innovation and Universities (FPU23/04128).

Author Contribution Kai L. Baltrusch: Conceptualization, Writing – original draft, Writing – review & editing, Methodology, Investigation, Formal analysis, Data curation. M. Dolores Torres: Conceptualization, Writing – review & editing, Formal analysis, Data curation., Validation, Supervision, Funding acquisition. Herminia Domínguez: Conceptualization, Writing – review & editing, Supervision, Funding acquisition.

Funding Funding for open access publishing: Universidade de Vigo /CISUG.

Availability of data and materials Data will be provided on request.

Declarations

Competing Interests The authors declare no competing interests.

Open Access This article is licensed under a Creative Commons Attribution 4.0 International License, which permits use, sharing, adaptation, distribution and reproduction in any medium or format, as long as you give appropriate credit to the original author(s) and the source, provide a link to the Creative Commons licence, and indicate if changes were made. The images or other third party material in this article are included in the article's Creative Commons licence, unless indicated otherwise in a credit line to the material. If material is not included in the article's Creative Commons licence and your intended use is not permitted by statutory regulation or exceeds the permitted use, you will need to obtain permission directly from the copyright holder. To view a copy of this licence, visit http://creativecommons.org/licenses/by/4.0/.

References

Abdul Khalil HPS, Lai TK, Tye YY, Rizal S, Chong EWN, Yap SW, Hamzah AA, Nurul MR, Paridah MT (2018) A review of extractions of seaweed hydrocolloids: properties and applications. Express Polym Lett 12:296–317

Andrade LR, Leal RN, Noseda M, Duarte MER, Pereira MS, Mourão PAS, Farina M, Amado FGM (2010) Brown algae overproduce cell wall polysaccharides as a protection mechanism against the heavy metal toxicity. Mar Pollut Bull 60:1482–1488

Andryukov BG, Besednova NN, Kuznetsova TA, Zaporozhets TS, Ermakova SP, Zvyagintseva TN, Chingizova EA, Gazha AK, Smolina TP (2020) Sulfated polysaccharides from marine algae as a basis of modern biotechnologies for creating wound dressings: current achievements and future prospects. Biomedicines 8:301

Azevedo G, Hilliou L, Bernardo G, Sousa-Pinto I, Adams RW, Nilsson M, Villanueva RD (2013) Tailoring kappa/iota-hybrid carrageenan from *Mastocarpus stellatus* with desired gel quality through pre-extraction alkali treatment. Food Hydrocoll 31:94–102

Azevedo G, Torres MD, Almeida PL, Hilliou L (2022) Exploring relationships between seaweeds carrageenan contents and extracted hybrid carrageenan properties in wild and cultivated *Mastocarpus stellatus*, *Chondrus crispus* and *Ahnfeltiopsis devoniensis*. Algal Res 67:102840

Baltrusch KL, Torres MD, Domínguez H (2024) Characterization, ultrafiltration, depolymerization and gel formulation of ulvans extracted via a novel ultrasound-enzyme assisted method. Ultrason Sonochem 111:107072

Baltrusch KL, Torres MD, Domínguez H (2025) Optimizing ultrasound-assisted extraction with custom design and response surface methodology: a case study using *Ulva* spp. Ultrason Sonochem 120:107443

Bianchi A, Sanz V, Domínguez H, Torres MD (2022) Valorisation of the industrial hybrid carrageenan extraction wastes using eco-friendly treatments. Food Hydrocoll 122:107070

Blanco-Pascual N, Alemán A, Gómez-Guillén MC, Montero MP (2014) Enzyme-assisted extraction of κ/ι-hybrid carrageenan from *Mastocarpus stellatus* for obtaining bioactive ingredients and their application for edible active film development. Food Funct 5:319–329

Cheng C, Cheng S, Su J, Zhu M, Zhou M, Chen T, Han Y (2022) Recent advances in carrageenan-based films for food packaging applications. Front Nutr 9:1004588

de Araújo CA, Noseda MD, Cipriani TR, Gonçalves AG, Duarte MER, Ducatti DRB (2013) Selective sulfation of carrageenans and the influence of sulfate regiochemistry on anticoagulant properties. Carbohydr Polym 91:483–49

Domozych DS, Ciancia M, Fangel JU, Mikkelsen MD, Ulvskov P, Willats WGT (2012) The cell walls of green algae: a journey through evolution and diversity. Front Plant Sci 3:82

Ellilä S, Fonseca L, Uchima C, Cota J, Goldman GH, Saloheimo M, Sacon V, Siika-Aho M (2017) Development of a low-cost cellulase production process using *Trichoderma reesei* for Brazilian biorefineries. Biotechnol Biofuels 10:30

Farshidfar N, Iravani S, Varma RS (2023) Alginate-based biomaterials in tissue engineering and regenerative medicine. Mar Drugs 21:189

Ferdiansyah R, Abdassah M, Zainuddin A, Rachmaniar R, Chaerunisaa AY (2023) Effects of alkaline solvent type and pH on solid physical properties of carrageenan from *Eucheuma cottonii*. Gels 9:397

Flórez-Fernández N, Falqué E, Domínguez H, Torres MD (2022) Green extraction of carrageenans from *Mastocarpus stellatus*. Polymers 14:554

Hettle AG, Vickers C, Robb CS, Liu F, Withers SG, Hehemann JH, Boraston AB (2018) The molecular basis of polysaccharide sulfatase activity and a nomenclature for catalytic subsites in this class of enzyme. Structure 26:747–758

Hilliou L, Larotonda FDS, Abreu P, Ramos AM, Sereno AM, Gonçalves MP (2006) Effect of extraction parameters on the chemical structure and gel properties of κ/ι-hybrid carrageenans obtained from *Mastocarpus stellatus*. Biomol Eng 23:201–208

Huang H, Wang Q, Ning Z, Ma Y, Huang Y, Wu Y, Yang Y, Xiao M, Ye J (2024) Preparation, antibacterial activity, and structure-activity relationship of low molecular weight κ-carrageenan. Int J Biol Macromol 266:131021

ICF International (2011) Carrageenan (Handling/Processing): Technical evaluation report. USDA National Organic Program, Washington. https://www.ams.usda.gov/sites/default/files/media/Carrageenan%20TR%202_10_16.pdf Accessed 11 Oct 2025

Li R, Xing R, Li H, Ren J, Chen L, Yu Z, Zhang H, Wu W, Li C, Zhu L, Cao X (2025) From terrestrial plants to marine macroalgae: a comprehensive review of cell wall component-properties, extraction, modification, and application of algal cellulose. J Agric Food Chem 73:23759–23782

Lomartire S, Gonçalves AMM (2023) Algal phycocolloids: bioactivities and pharmaceutical applications. Mar Drugs 21:384

Lourenço SO, Barbarino E, De-Paula JC et al (2002) Amino acid composition, protein content and calculation of nitrogen-to-protein conversion factors for 19 tropical seaweeds. Phycol Res 50:233–241

Matos GS, Pereira SG, Genisheva ZA, Gomes AM, Teixeira JA, Rocha CMR (2021) Advances in extraction methods to recover added-value compounds from seaweeds: sustainability and functionality. Foods 10:516

Mendes M, Cotas J, Gutiérrez IB, Gonçalves AMM, Critchley AT, Hinaloc LAR, Roleda MY, Pereira L (2024) Advanced extraction techniques and physicochemical properties of carrageenan from a novel *Kappaphycus alvarezii* cultivar. Mar Drugs 22:291

Meroni D, Djellabi R, Ashokkumar M, Bianchi CL, Boffito DC (2022) Sonoprocessing: from concepts to large-scale reactors. Chem Rev 122:3219–3258

Michel G, Tonon T, Scornet D, Cock JM, Kloareg B (2010) Central and storage carbon metabolism of the brown alga *Ectocarpus siliculosus*: insights into the origin and evolution of storage carbohydrates in eukaryotes. New Phytol 188:67–81

Miller IJ, Blunt JW (2002) Evaluation of the structure of the polysaccharides from *Chondria macrocarpa* and *Ceramium rubrum* as determined by ^{13}C NMR spectroscopy. Bot Mar 45:1–8

Morelli A, Puppi D, Chiellini F (2017) Perspectives on biomedical applications of ulvan. In: Venkatesan J, Anil S, Kim S-K (eds) Seaweed Polysaccharides. Isolation, Biological and Biomedical Applications. Elsevier, Amsterdam, pp 305–330

Olofsson J, Barta Z, Börjesson P, Wallberg O (2015) Life cycle assessment and techno-economical analysis of on-site enzyme production in 2nd generation bioethanol. Report No. 2015:05, f3. The Swedish Knowledge Centre for Renewable Transportation Fuels, Sweden. https://f3centre.se/app/uploads/f3_report_2015-05_Enzyme-production-in-2nd-generation-bioethanol-150925.pdf. Accessed 11 Oct 2025

Olofsson J, Barta Z, Börjesson P, Wallberg O (2017) Integrating enzyme fermentation in lignocellulosic ethanol production: life-cycle assessment and techno-economic analysis. Biotechnol Biofuels 10:51

Ørsted (2017) Residues from Novo Nordisk and Novozymes converted into biogas. https://stateofgreen.com/en/news/residues-from-novo-nordisk-and-novozymes-converted-into-biogas/. Accessed 11 Oct 2025

Patel S (2012) Therapeutic importance of sulfated polysaccharides from seaweeds: updating the recent findings. 3 Biotech 2:171–185

Pereira L, Van De Velde F (2011) Portuguese carrageenophytes: carrageenan composition and geographic distribution of eight species (Gigartinales, Rhodophyta). Carbohydr Polym 84:614–623

Pereira L, Amado AM, Critchley AT, de Van Vel F, Ribeiro-Claro PJA (2009) Identification of selected seaweed polysaccharides (phycocolloids) by vibrational spectroscopy (FTIR-ATR and FT-Raman). Food Hydrocoll 23:1903–1909

Prado-Fernández J, Rodríguez-Vázquez JA, Tojo E, Andrade JM (2003) Quantitation of κ-, ι- and λ-carrageenans by mid-infrared spectroscopy and PLS regression. Anal Chim Acta 480:23–37

Qiu SM, Aweya JJ, Liu X, Liu Y, Tang S, Zhang W, Cheong KL (2022) Bioactive polysaccharides from red seaweed as potent food supplements: a systematic review of their extraction, purification, and biological activities. Carbohydr Polym 275:118696

Ramos-de-la-Peña AM, Contreras-Esquivel JC, Aguilar O, González-Valdez J (2022) Structural and bioactive roles of fucoidan in nanogel delivery systems. A review. Carbohydr Polym Technol Applic 4:100235

Rhein-Knudsen N, Reyes-Weiss D, Horn SJ (2023) Extraction of high purity fucoidans from brown seaweeds using cellulases and alginate lyases. Int J Biol Macromol 229:199–209

Rochas C, Lahaye M, Yaphe W (1986) Sulfate content of carrageenan and agar determined by infrared spectroscopy. Bot Mar 29:335–340

Sabu Mathew S, Jaiswal AK, Jaiswal S (2024) Carrageenan-based sustainable biomaterials for intelligent food packaging: a review. Carbohydr Polym 342:122267

Sarkar S, Gayen K, Bhowmick TK (2022) Green extraction of biomolecules from algae using subcritical and supercritical fluids. Biomass Convers Biorefin 15:21603–21625

Sfriso AA, Gallo M, Baldi F (2017) Seasonal variation and yield of sulfated polysaccharides in seaweeds from the Venice Lagoon. Bot Mar 60:339–349

Shen S, Chen X, Shen Z, Chen H (2021) Marine polysaccharides for wound dressings application: an overview. Pharmaceutics 13:1666

Shepherd VA, Beilby MJ, Heslop DJ (1999) Ecophysiology of the hypotonic response in the salt-tolerant charophyte alga *Lamprothamnium papulosum*. Plant Cell Environ 22:333–346

Silveira MHL, Chandel AK, Vanelli BA, Sacilotto KS, Cardoso EB (2018) Production of hemicellulosic sugars from sugarcane bagasse via steam explosion employing industrially feasible conditions: pilot scale study. Bioresour Technol Rep 3:138–146

Skriptsova AV (2016) Seasonal variations in the fucoidan content of brown algae from Peter the Great Bay, Sea of Japan. Russ J Mar Biol 42:351–356

Tasende MG, Cid M, Fraga MI (2013) Qualitative and quantitative analysis of carrageenan content in gametophytes of *Mastocarpus stellatus* (Stackhouse) Guiry along Galician coast (NW Spain). J Appl Phycol 25:587–596

The European Commission (2021) Comission Implementing Regulation (EU) 2021/1165 of 15 July 2021 authorising certain products and substances for use in organic production and establishing their lists. Off J Eur Union 91:13–48

Torres MD, Flórez-Fernández N, Domínguez H (2021) Ultrasound-assisted water extraction of *Mastocarpus stellatus* carrageenan with adequate mechanical and antiproliferative properties. Mar Drugs 19:280

US Department of Agriculture (2023) https://www.ams.usda.gov/rules regulations/organic/petitioned-substances/carrageenan

U.S. Department of Agriculture (2025) National Organic Program: 7 CFR Part 205. Agricultural Marketing Service. U. S. Food and Drug Administration, Washington. https://www.ecfr.gov/current/title-7/subtitle-B/chapter-I/subchapter-M/part-205. Accessed 11 Oct 2025

US Food Drug Administration (2020) GRAS Notice No. GRN 000891. U.S. Department of Health and Human Services, Washington. https://hfpappexternal.fda.gov/scripts/fdcc/index.cfm?set=GRASNotices&id=891&sort=GRN_No&order=DESC&startrow=1&type=basic&search=891. Accessed 11 Oct 2025

U.S. Food and Drug Administration (2025) Carrageenan. 21 CFR §172.620. US Department of Health and Human Services, Washington. https://www.ecfr.gov/current/title-21/chapter-I/subchapter-B/part-172/subpart-G/section-172.620. Accessed 11 Oct 2025

US Food and Drug Administration (2025) https://www.fda.gov/food/food-ingredients-packaging/generally-recognized-safe-gras

Van De Velde F, Peppelman HA, Rollema HS, Hans R (2001) On the structure of κ/ι-hybrid carrageenans. Carbohydr Res 331:271–283

Van De Velde F, Knutsen SH, Usov AI, Rollema HS, Cerezo AS (2002) ^{1}H and ^{13}C high resolution NMR spectroscopy of carrageenans: application in research and industry. Trends Food Sci Technol 13:73–92

Van De Velde F, Pereira L, Rollema HS (2004) The revised NMR chemical shift data of carrageenans. Carbohydr Res 339:2309–2313

Zhang J, Langford Z, Waldron S (2023) The global carrageenan industry. In: Langford Z (ed) Globalisation and Livelihood Transformations in the Indonesian Seaweed Industry. Routledge, London, pp 23–50

Publisher's Note Springer Nature remains neutral with regard to jurisdictional claims in published maps and institutional affiliations.